What we can learn from the angular differential rates from semileptonic $B \to D^* \ell \nu_\ell$ decays

G. Martinelli,[1] S. Simula,[2] and L. Vittorio[3]

[1]*Physics Department and INFN Sezione di Roma La Sapienza, Piazzale Aldo Moro 5, 00185 Roma, Italy*
[2]*Istituto Nazionale di Fisica Nucleare, Sezione di Roma Tre, Via della Vasca Navale 84, I-00146 Rome, Italy*
[3]*LAPTh, Université Savoie Mont-Blanc and CNRS, F-74941 Annecy, France*

(Received 25 September 2024; accepted 2 January 2025; published 22 January 2025)

We present a simple approach to the study of semileptonic $B \to D^* \ell \nu_\ell$ decays based on the angular distributions of the final state particles only. Our approach is model independent and never requires the knowledge of $|V_{cb}|$. By studying such distributions in the case of light leptons, a comparison between results from different datasets from the Belle and BelleII Collaborations and between data and Standard Model calculations is also given for several interesting quantities. A good consistency is observed between some of the experimental results and the theoretical predictions.

DOI: 10.1103/PhysRevD.111.013005

I. INTRODUCTION

In this work we discuss a straightforward approach to the analysis of semileptonic $B \to D^* \ell \nu_\ell$ decays based on the angular distributions of the final state particles. Although several analyses which make use of the angular distributions already exist in the literature [1–13], our study as well as the one in Ref. [14] are only based on the angular distributions and reduce the problem to the determination of few basic parameters (five in all). These parameters encode in the most general way the contributions to the differential decay rates coming from operators present in the effective Hamiltonian either in the Standard Model (SM) or from physics Beyond the Standard Model (BSM). The analysis is model independent and never requires the knowledge of $|V_{cb}|$. In this work we analyze for the first time the angular distributions of different experimental datasets. This allows a direct comparison of the results obtained from different experiments as well as with the theoretical predictions based on the hadronic form factors (FFs) obtained from available lattice QCD (LQCD) simulations. While in some specific cases differences (within about two standard deviations) are visible, a quite good consistency is observed between some of the experimental results and the theoretical predictions of the SM using the LQCD FFs. The present study is limited to $B \to D^* \ell \nu_\ell$ decays with light leptons in the final states, for which possible BSM contributions have been considered in the past [7,15] and also more recently [11,13,16].

Using the most general structure of the fourfold differential decay rate for semileptonic $B \to D^* \ell \nu_\ell$ decays, the five basic parameters (denoted in the following as $\{\eta, \eta', \delta, \epsilon, \epsilon'\}$) are defined in terms of experimentally measurable quantities related to different angular distributions, which will be the basis of our phenomenological analysis, namely,

$$\frac{1}{\Gamma}\frac{d\Gamma}{d\cos\theta_v} = \frac{3}{4(1+\eta)}\{\eta + (2-\eta)\cos^2\theta_v\}, \tag{1}$$

$$\frac{1}{\Gamma}\frac{d\Gamma}{d\cos\theta_\ell} = \frac{3}{8(1+\eta')} \times \{2 + \eta' - 2\delta\cos\theta_\ell - (2-\eta')\cos^2\theta_\ell\}, \tag{2}$$

$$\frac{1}{\Gamma}\frac{d\Gamma}{d\chi} = \frac{1}{2\pi}\left\{1 - \frac{\epsilon}{1+\eta}\cos 2\chi - \frac{\epsilon'}{1+\eta}\sin 2\chi\right\}. \tag{3}$$

In order to disentangle δ from η', a separation of the dependence of $1/\Gamma d\Gamma/d\cos\theta_\ell$ on the even or odd terms in $\cos\theta_\ell$ is necessary. In literature it is common to refer to observables like the forward-backward asymmetry A_{FB}, the longitudinal D^*-polarization fraction F_L, and the two transverse asymmetries A_{1c} and A_{9c}.[1] These quantities are related to the five hadronic parameters $\{\eta, \eta', \delta, \epsilon, \epsilon'\}$ by

[1]The asymmetries A_{1c} and A_{9c} correspond to the quantities S_3 and S_9, respectively, as defined in Ref. [17], multiplied by π. A_{9c} corresponds to $A_T^{(1)}$ defined in Eq. (37) of Ref. [4].

$$A_{FB} = -\frac{3}{4}\frac{\delta}{1+\eta'}, \tag{4}$$

$$F_L = \frac{1}{1+\eta}, \tag{5}$$

$$A_{1c} = -\frac{\epsilon}{1+\eta}, \tag{6}$$

$$A_{9c} = -\frac{\epsilon'}{1+\eta}, \tag{7}$$

and will be used in the present analysis.

The plan of the remainder of the paper is the following: in Sec. II we recall the most general expression of the $B \to D^*$ differential decay rate in the momentum transfer and in the relevant angular variables. We then derive the expressions given in Eqs. (1)–(7); in Sec. III we express the basic parameters $\{\eta, \eta', \delta, \epsilon, \epsilon'\}$ in terms of the helicity amplitudes computed in the SM; in Sec. IV we describe our fit of the data from different measurements, present tables and figures containing the results, and discuss their compatibility and consistency with the SM. The final section contains our conclusions.

II. THE FOURFOLD $B \to D^*$ DIFFERENTIAL DECAY RATE AND THE DEFINITION OF THE BASIC PARAMETERS

In this section we derive the expressions in Eqs. (1)–(3) from the fourfold $B \to D^*$ differential decay rate. The general structure of the fourfold differential rate for $B \to D^* \ell \nu_\ell$ decays, valid both within the SM and including possible BSM effects, can be expressed in terms of 12 angular observables (coefficients) $J_i(w)$ [3,4,15,17], functions of the recoil variable w, which is given in terms of the squared four-momentum transfer q^2 by

$$w \equiv \frac{1 + r^2 - q^2/m_B^2}{2r} \tag{8}$$

with $r \equiv m_{D^*}/m_B$. The dependence on the squared momentum transfer is all condensed in the angular observables themselves, which can be expressed in terms of the helicity amplitudes (and then in terms of the hadronic FFs) and of the Wilson coefficients of the relevant operators as done in Refs. [3,4] (very detailed and complementary discussions can be also found in Refs. [1,5]). The physical quantities $J_i(w)$ are particularly relevant to scrutinize the presence of BSM effects in semileptonic $B \to D^*$ decays. Following the notation of Ref. [17], one has[2]

$$\begin{aligned}\frac{d^4\Gamma(B \to D^* \ell \nu_\ell)}{dw\, d\cos\theta_v\, d\cos\theta_\ell\, d\chi} = \frac{3}{16\pi}\Gamma_0 \{ & J_{1s}(w)\sin^2\theta_v + J_{1c}(w)\cos^2\theta_v + J_{2s}(w)\sin^2\theta_v \cos 2\theta_\ell + J_{2c}(w)\cos^2\theta_v \cos 2\theta_\ell \\ & + J_3(w)\sin^2\theta_v \sin^2\theta_\ell \cos 2\chi + J_4(w)\sin 2\theta_v \sin 2\theta_\ell \cos\chi + J_5(w)\sin 2\theta_v \sin\theta_\ell \cos\chi \\ & + J_{6s}(w)\sin^2\theta_v \cos\theta_\ell + J_{6c}(w)\cos^2\theta_v \cos\theta_\ell + J_7(w)\sin 2\theta_v \sin\theta_\ell \sin\chi \\ & + J_8(w)\sin 2\theta_v \sin 2\theta_\ell \sin\chi + J_9(w)\sin^2\theta_v \sin^2\theta_\ell \sin 2\chi \},\end{aligned} \tag{9}$$

where

$$\Gamma_0 \equiv \frac{\eta_{EW}^2 m_B m_{D^*}^2}{(4\pi)^3} G_F^2 |V_{cb}|^2 \tag{10}$$

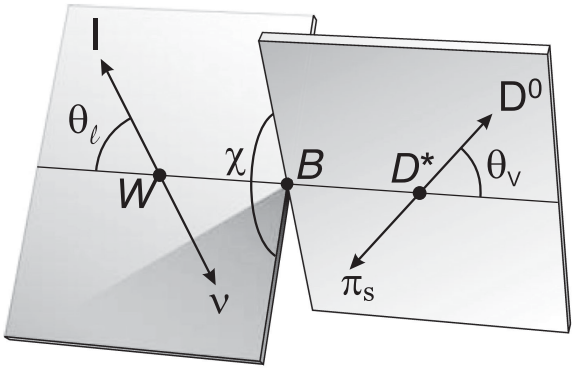

FIG. 1. Definition of the angles θ_v, θ_ℓ, and χ for the decay $B \to D^*(D\pi)\ell\nu_\ell$. This figure has been taken from Ref. [18].

with $\eta_{EW} = 1.0066$, G_F the Fermi constant, and V_{cb} the relevant Cabibbo-Kobayashi-Maskawa matrix element. The angles θ_v, θ_ℓ, and χ are defined as in Fig. 1.

The total decay rate is given by

$$\Gamma(B \to D^* \ell \nu_\ell) = \frac{1}{6}\Gamma_0 [6\bar{J}_{1s} + 3\bar{J}_{1c} - 2\bar{J}_{2s} - \bar{J}_{2c}], \tag{11}$$

where the quantities $\bar{J}_i$ are the integrated angular coefficients over the full kinematical range of w, namely,

$$\bar{J}_i \equiv \int_1^{w_{\max}^\ell} dw J_i(w) \tag{12}$$

with

[2]The angular coefficients $J_i(w)$, defined in Eq. (9), are proportional to the corresponding ones defined in Ref. [17] by a multiplicative constant equal to $2^{10} m_B^3/3m_{D^*}$.

$$w_{\rm max}^{\ell} \equiv \frac{1+r^2-m_\ell^2/m_B^2}{2r}. \tag{13}$$

By dividing Eq. (9) by the total rate Γ, one gets the fourfold decay ratio independent of V_{cb}, namely,

$$\begin{aligned}\frac{1}{\Gamma}\frac{d^4\Gamma(B\to D^*\ell\nu_\ell)}{dw\,d\cos\theta_v\,d\cos\theta_\ell\,d\chi} = \frac{1}{\mathcal{N}}\{&J_{1s}(w)\sin^2\theta_v + J_{1c}(w)\cos^2\theta_v + J_{2s}(w)\sin^2\theta_v\cos 2\theta_\ell + J_{2c}(w)\cos^2\theta_v\cos 2\theta_\ell\\ &+ J_3(w)\sin^2\theta_v\sin^2\theta_\ell\cos 2\chi + J_4(w)\sin 2\theta_v\sin 2\theta_\ell\cos\chi + J_5(w)\sin 2\theta_v\sin\theta_\ell\cos\chi\\ &+ J_{6s}(w)\sin^2\theta_v\cos\theta_\ell + J_{6c}(w)\cos^2\theta_v\cos\theta_\ell + J_7(w)\sin 2\theta_v\sin\theta_\ell\sin\chi\\ &+ J_8(w)\sin 2\theta_v\sin 2\theta_\ell\sin\chi + J_9(w)\sin^2\theta_v\sin^2\theta_\ell\sin 2\chi\},\end{aligned} \tag{14}$$

where

$$\mathcal{N} = \frac{8\pi}{9}[6\bar{J}_{1s} + 3\bar{J}_{1c} - 2\bar{J}_{2s} - \bar{J}_{2c}]. \tag{15}$$

After integrating Eq. (14) over the recoil variable w and over two out of the three angular coordinates $\{\theta_v, \theta_\ell, \chi\}$, we obtain the single-differential angular decay rates

$$\begin{aligned}\frac{1}{\Gamma}\frac{d\Gamma}{d\cos\theta_v} = \frac{4\pi}{3\mathcal{N}}\{&3\bar{J}_{1s} - \bar{J}_{2s}\\ &+ (3\bar{J}_{1c} - \bar{J}_{2c} - 3\bar{J}_{1s} + \bar{J}_{2s})\cos^2\theta_v\},\end{aligned} \tag{16}$$

$$\begin{aligned}\frac{1}{\Gamma}\frac{d\Gamma}{d\cos\theta_\ell} = \frac{4\pi}{3\mathcal{N}}\{&2\bar{J}_{1s} - 2\bar{J}_{2s} + \bar{J}_{1c} - \bar{J}_{2c}\\ &+ (2\bar{J}_{6s} + \bar{J}_{6c})\cos\theta_\ell + 2(2\bar{J}_{2s} + \bar{J}_{2c})\cos^2\theta_\ell\},\end{aligned} \tag{17}$$

$$\frac{1}{\Gamma}\frac{d\Gamma}{d\chi} = \frac{1}{2\pi}\left\{1 + \frac{32\pi}{9\mathcal{N}}\bar{J}_3\cos 2\chi + \frac{32\pi}{9\mathcal{N}}\bar{J}_9\sin 2\chi\right\}. \tag{18}$$

By defining the following dimensionless quantities

$$\eta \equiv 2\frac{3\bar{J}_{1s} - \bar{J}_{2s}}{3\bar{J}_{1c} - \bar{J}_{2c}}, \tag{19}$$

$$\eta' \equiv 2\frac{2\bar{J}_{1s} + \bar{J}_{1c} + 2\bar{J}_{2s} + \bar{J}_{2c}}{2\bar{J}_{1s} + \bar{J}_{1c} - 3(2\bar{J}_{2s} + \bar{J}_{2c})}, \tag{20}$$

$$\delta = -2\frac{2\bar{J}_{6s} + \bar{J}_{6c}}{2\bar{J}_{1s} + \bar{J}_{1c} - 3(2\bar{J}_{2s} + \bar{J}_{2c})}, \tag{21}$$

$$\epsilon \equiv -4\frac{\bar{J}_3}{3\bar{J}_{1c} - \bar{J}_{2c}}, \tag{22}$$

$$\epsilon' \equiv -4\frac{\bar{J}_9}{3\bar{J}_{1c} - \bar{J}_{2c}}, \tag{23}$$

we get the expressions in Eqs. (1)–(3).

Therefore, even including BSM effects (cf. also Refs. [14,19]), the single-differential angular decay rates (1)–(3) have a precise dependence on the angular coordinates $\{\theta_v, \theta_\ell, \chi\}$ governed only by five hadronic parameters given by $\{\eta, \eta', \delta, \epsilon, \epsilon'\}$, defined by Eqs. (19)–(23) in terms of the integrated angular coefficients $\bar{J}_i$. The quantities A_{FB}, F_L, A_{1c}, and A_{9c} can be easily derived from Eqs. (1)–(3) obtaining Eqs. (4)–(7).

III. THE ANGULAR VARIABLES $J_i(w)$ IN THE SM

Within the SM the angular coefficients $J_i(w)$ can be expressed in terms of the helicity amplitudes $H_{+,-,0,t}(w)$ [17] as

$$J_{1s}(w) = \frac{3}{2}F(w)[H_+^2(w) + H_-^2(w)]\left(1 + \frac{m_\ell^2}{3q^2}\right), \tag{24}$$

$$J_{1c}(w) = 2F(w)\left[H_0^2(w)\left(1 + \frac{m_\ell^2}{q^2}\right) + 2\frac{m_\ell^2}{q^2}H_t^2(w)\right], \tag{25}$$

$$J_{2s}(w) = \frac{1}{2}F(w)[H_+^2(w) + H_-^2(w)]\left(1 - \frac{m_\ell^2}{q^2}\right), \tag{26}$$

$$J_{2c}(w) = -2F(w)H_0^2(w)\left(1 - \frac{m_\ell^2}{q^2}\right), \tag{27}$$

$$J_3(w) = -2F(w)H_+(w)H_-(w)\left(1 - \frac{m_\ell^2}{q^2}\right), \tag{28}$$

$$J_4(w) = F(w)H_0(w)[H_+(w) + H_-(w)]\left(1 - \frac{m_\ell^2}{q^2}\right), \tag{29}$$

$$\begin{aligned}J_5(w) = 2F(w)\Big\{&H_0(w)[H_-(w) - H_+(w)]\\ &+ \frac{m_\ell^2}{q^2}H_t(w)[H_+(w) + H_-(w)]\Big\},\end{aligned} \tag{30}$$

$$J_{6s}(w) = -2F(w)[H_+^2(w) - H_-^2(w)], \tag{31}$$

$$J_{6c}(w) = -8\frac{m_\ell^2}{q^2}F(w)H_0(w)H_t(w), \tag{32}$$

$$J_7(w) = J_8(w) = J_9(w) = 0, \tag{33}$$

where the kinematical factor $F(w)$ is given by

$$F(w) \equiv \sqrt{w^2-1}(1+r^2-2rw)\qquad\left(1-\frac{m_\ell^2}{q^2}\right)^2. \tag{34}$$

It follows that, within the SM, the quantities $\{\eta, \eta', \delta, \epsilon, \epsilon'\}$ are explicitly given by

$$\eta = \frac{H_{++}+H_{--}+\frac{m_\ell^2}{2m_B^2}(\tilde{H}_{++}+\tilde{H}_{--})}{H_{00}+\frac{m_\ell^2}{2m_B^2}(\tilde{H}_{00}+3\tilde{H}_{tt})}, \tag{35}$$

$$\eta' = \frac{H_{++}+H_{--}+\frac{m_\ell^2}{m_B^2}(\tilde{H}_{00}+\tilde{H}_{tt})}{H_{00}+\frac{m_\ell^2}{2m_B^2}(\tilde{H}_{++}+\tilde{H}_{--}-\tilde{H}_{00}+\tilde{H}_{tt})}, \tag{36}$$

$$\delta = \frac{H_{++}-H_{--}+\frac{2m_\ell^2}{m_B^2}\tilde{H}_{0t}}{H_{00}+\frac{m_\ell^2}{2m_B^2}(\tilde{H}_{++}+\tilde{H}_{--}-\tilde{H}_{00}+\tilde{H}_{tt})}, \tag{37}$$

$$\epsilon = \frac{H_{+-}-\frac{m_\ell^2}{m_B^2}\tilde{H}_{+-}}{H_{00}+\frac{m_\ell^2}{2m_B^2}(\tilde{H}_{00}+3\tilde{H}_{tt})}, \tag{38}$$

$$\epsilon' = 0, \tag{39}$$

where for $i, j = \{+, -, 0, t\}$

$$H_{ij} \equiv \int_1^{w_{\max}^\ell} dw\sqrt{w^2-1}(1-2rw+r^2) \times\left(1-\frac{m_\ell^2}{q^2}\right)^2 H_i(w)H_j(w), \tag{40}$$

$$\tilde{H}_{ij} \equiv \int_1^{w_{\max}^\ell} dw\sqrt{w^2-1}\left(1-\frac{m_\ell^2}{q^2}\right)^2 H_i(w)\,H_j(w). \tag{41}$$

Note that, if we neglect the mass of the final charged lepton, we have $\eta' = \eta$ and the four quantities A_{FB}, F_L, A_{1c}, and A_{9c} are sufficient to determine all the basic parameters.

The helicity amplitudes $H_{+,-,0,t}(w)$ are related to the standard FFs $f(w)$, $g(w)$, $F_1(w)$, and $F_2(w)$ of Ref. [20], corresponding to definite spin parity (to which the unitarity bounds can be applied), by

$$H_+(w) = f(w) - m_B^2 r\sqrt{w^2-1}g(w), \tag{42}$$

$$H_-(w) = f(w) + m_B^2 r\sqrt{w^2-1}g(w), \tag{43}$$

$$H_0(w) = \frac{F_1(w)}{m_B\sqrt{1-2rw+r^2}}, \tag{44}$$

$$H_t(w) = \frac{m_B r\sqrt{w^2-1}}{\sqrt{1-2rw+r^2}}F_2(w). \tag{45}$$

In what follows, we make use of the FFs obtained in Ref. [21] by applying the unitary dispersive matrix (DM) approach [22] to all available LQCD results determined by FNAL/MILC [23], HPQCD [24], and JLQCD [25] Collaborations. With the above FFs we calculate the helicity amplitudes $H_{+,-,0,t}(w)$ in the full kinematical range of w (i.e., $1 \le w \le w_{\max}^\ell$) and, consequently, the hadronic parameters $\{\eta, \eta', \delta, \epsilon\}$ through Eqs. (19)–(22), as well as the asymmetries A_{FB}, F_L, A_{1c} through Eqs. (4)–(6). Within the SM, one has $\epsilon' = 0$ and, consequently, $A_{9c} = 0$.

IV. FIT OF THE DATA AND DISCUSSION OF THE RESULTS

We now consider the three experimental datasets directly available for the single-differential decay rates $d\Gamma/dx$, where $x = \{\cos\theta_\ell, \cos\theta_v, \chi\}$, from Refs. [18,26,27], which hereafter will be labeled as Belle18, Belle23, and BelleII23, respectively. For the sake of precision, only for Belle23 and BelleII23 the datasets are available directly for the ratios $(1/\Gamma)d\Gamma/dx$, while for Belle18 Ref. [18] provides the efficiencies and response functions necessary to unfold the measured binned yields. Using Monte Carlo samplings for propagating all the experimental uncertainties we have unfolded the data of Ref. [18], obtaining in this way the values of $d\Gamma/dx$ for each experimental bin, including the corresponding covariance matrix. Our results are well consistent with those shown in Refs. [9,19,23–25], For the present discussion we do not need the fourth differential decay rate $d\Gamma/dw$.

Thus, the Belle18 [18] and Belle23 [26] experimental data are given in the form of ten-bin distributions for each of the three kinematical variables $x = \{\cos\theta_l, \cos\theta_v, \chi\}$, namely,

$$\Delta\Gamma_n^x = \int_{x_{n-1}}^{x_n} dx'\frac{d\Gamma}{dx'}, \qquad n = 1, 2, \ldots 10 \tag{46}$$

with

$$\begin{aligned}
\{(\cos\theta_v)_n\} &= \{-1, -0.8, -0.6, -0.4, -0.2, 0.0, 0.2, 0.4, 0.6, 0.8, 1.0\},\\
\{(\cos\theta_\ell)_n\} &= \{-1, -0.8, -0.6, -0.4, -0.2, 0.0, 0.2, 0.4, 0.6, 0.8, 1.0\},\\
\{\chi_n\} &= \left\{0, \frac{\pi}{5}, \frac{2\pi}{5}, \frac{3\pi}{5}, \frac{4\pi}{5}, \pi, \frac{6\pi}{5}, \frac{7\pi}{5}, \frac{8\pi}{5}, \frac{9\pi}{5}, 2\pi\right\}.
\end{aligned} \tag{47}$$

TABLE I. Results obtained for the five hadronic parameters $\{\eta, \eta', \delta, \epsilon, \epsilon'\}$, describing the dependence of the ratios (50)–(52) on the experimental bins of the Belle18 [18], Belle23 [26], and BelleII23 [27] datasets. The row denoted by Belle18 + Belle23 + BelleII23 corresponds to the results obtained using simultaneously all three experimental datasets. The row denoted as Belle23(Ji) shows the results corresponding to Eqs. (19)–(23) using the experimental results for the w-integrated angular coefficients $\bar{J}_i$ from Ref. [17]. The last row shows the SM predictions (35)–(39) obtained by using the hadronic FFs of the unitary DM approach of Ref. [21] based on all available LQCD results from FNAL/MILC [23], HPQCD [24], and JLQCD [25] collaborations. All of the results correspond to the averaged e/μ case.

	η	η'	δ	ϵ	ϵ'
Belle18	0.894 (29)	0.846 (47)	−0.534 (37)	0.346 (28)	0.004 (28)
Belle23	1.026 (59)	0.943 (81)	−0.595 (41)	0.333 (61)	0.046 (59)
BelleII23	0.912 (28)	0.908 (47)	−0.507 (28)	0.342 (22)	0.005 (19)
Belle18 + Belle23 + BelleII23	0.922 (18)	0.875 (29)	−0.540 (18)	0.337 (16)	0.005 (16)
Belle23(Ji)	1.097 (73)	0.934 (86)	−0.626 (49)	0.361 (69)	−0.054 (67)
LQCD	1.109 (66)	1.121 (66)	−0.705 (48)	0.415 (26)	0.0

The BelleII23 data [27] are given in the same ten bins for the variables $\cos\theta_v$ and χ, while in the case of $\cos\theta_\ell$ the BelleII23 bins are only eight, since the first BelleII23 bin corresponds to the sum of the first three Belle18 and Belle23 bins and the BelleII23 bins 2–8 correspond to the Belle18 and Belle23 bins 4–10. Thus, we have a total of $N = 30$ data points for both Belle18 and Belle23 and $N = 28$ data points for BelleII23, including the corresponding experimental covariance matrix of dimension $N \times N$.

For each kinematical variable x the sum over the bins covers the full kinematical range. Therefore, for each set of experimental data we consider the ratios

$$R_n^x \equiv \frac{1}{\sum_{m=1}^{N_x} \Delta\Gamma_m^x} \Delta\Gamma_n^x, \tag{48}$$

which should satisfy the normalization

$$\sum_{n=1}^{N_x} R_n^x = 1, \tag{49}$$

with N_x being the number of experimental bins for the variable x. For the case of Belle18, using multivariate Gaussian distributions for the experimental values of $\Delta\Gamma_n^x$, we construct the ratios (48) and evaluate also the corresponding covariance matrix $\mathbf{C}_{nm}$ $(n, m = 1, \ldots, N)$. Using the experimental bins (47) one has (for $n = 1, 2, \ldots, 10$)

$$R_n^{\theta_v} = \frac{3}{20(1+\eta)}\left[\eta + \frac{2-\eta}{75}(91 - 33n + 3n^2)\right], \tag{50}$$

$$R_n^{\theta_\ell} = \frac{3}{40(1+\eta')}\left[2 + \eta' - \frac{\delta}{5}(-11 + 2n) - \frac{2-\eta'}{75}(91 - 33n + 3n^2)\right], \tag{51}$$

$$R_n^{\chi} = \frac{1}{10} - \frac{1}{4\pi}\frac{\epsilon}{1+\eta}\left[\sin\frac{2n\pi}{5} - \sin\frac{2(n-1)\pi}{5}\right] - \frac{1}{4\pi}\frac{\epsilon'}{1+\eta}\left[\cos\frac{2(n-1)\pi}{5} - \cos\frac{2n\pi}{5}\right]. \tag{52}$$

For each experiment we can now extract the values of the five hadronic parameters $\{\eta, \eta', \delta, \epsilon, \epsilon'\}$ appearing in the above equations. This is obtained by performing a χ^2-minimization procedure based on a correlated χ^2. Since the covariance matrices $\mathbf{C}_{nm}$ are singular because of the conditions (49), we adopt the Moore-Penrose pseudoinverse approach, commonly used in least-square procedures. Since each of the matrices $\mathbf{C}_{nm}$ possesses three null eigenvalues, the total number of degrees of freedom is $N_{\rm dof} = N - 3$ for each experiment.

Our results, which always correspond to the averaged e/μ case, are presented in Table I for the basic parameters $\{\eta, \eta', \delta, \epsilon, \epsilon'\}$ (19)–(23) and in Table II in terms of the

TABLE II. Results for the quantities in Eqs. (4)–(7). The description of the different rows is the same as in Table I.

	A_{FB}	F_L	A_{1c}	A_{9c}
Belle18	0.217 (13)	0.528 (8)	−0.183 (15)	−0.002 (15)
Belle23	0.230 (14)	0.494 (14)	−0.165 (30)	−0.023 (29)
BelleII23	0.200 (12)	0.523 (8)	−0.179 (13)	−0.003 (10)
Belle18 + Belle23 + BelleII23	0.216 (7)	0.520 (5)	−0.176 (9)	−0.003 (8)
Belle23(Ji)	0.243 (14)	0.477 (17)	−0.172 (32)	0.003 (32)
LQCD	0.249 (10)	0.475 (15)	−0.196 (7)	0.0

quantities (4)–(7). These results are given separately for the three sets of experimental data (Belle18, Belle23, and BelleII23). In the two tables also other cases have been considered, namely,

(i) Belle18 + Belle23 + BelleII23: We extract the hadronic parameters $\{\eta, \eta', \delta, \epsilon, \epsilon'\}$ from Eqs. (50)–(52) using simultaneously all the three experimental datasets Belle18, Belle23, and BelleII23 for the ratios (which are not correlated among different experiments).

(ii) Belle23(Ji): We evaluate directly the hadronic parameters from Eqs. (19)–(23) using for the integrated angular coefficients $\bar{J}_i$ the sum of the experimental results in the four w bins adopted in Ref. [17]. In other words, using Eqs. (16)–(18) we construct a new dataset for the ratios (50)–(52), which will be referred to as Belle23(Ji). Note that the two sets Belle23 and Belle23(Ji) share the same fourfold differential dataset. They differ only in the

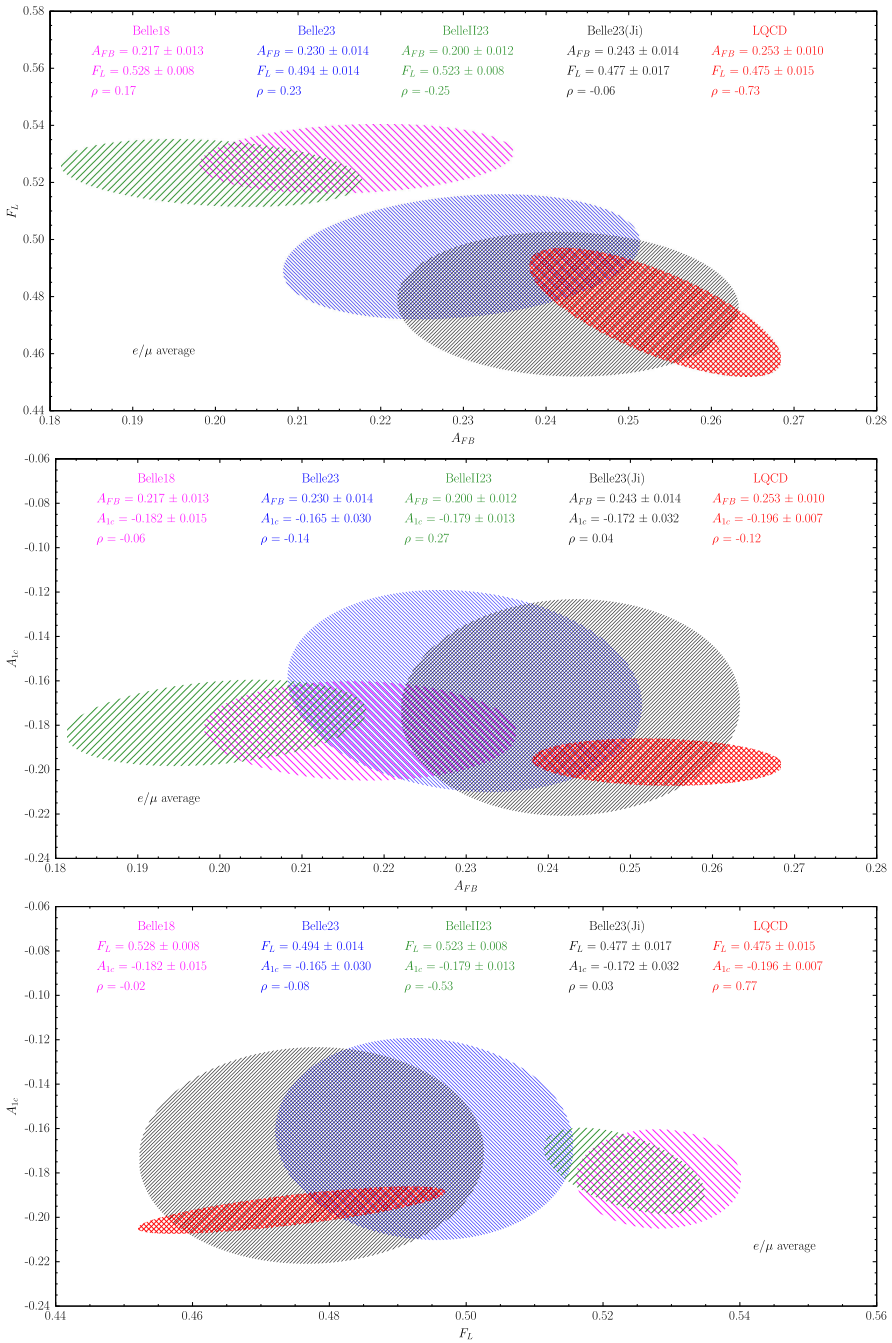

FIG. 2. Contour plots (at 68% probability) for the asymmetries A_{FB}, F_L, and A_{1c} corresponding to the analyses specified in the insets and given in Table II. In the insets the quantity ρ represents the correlation coefficient.

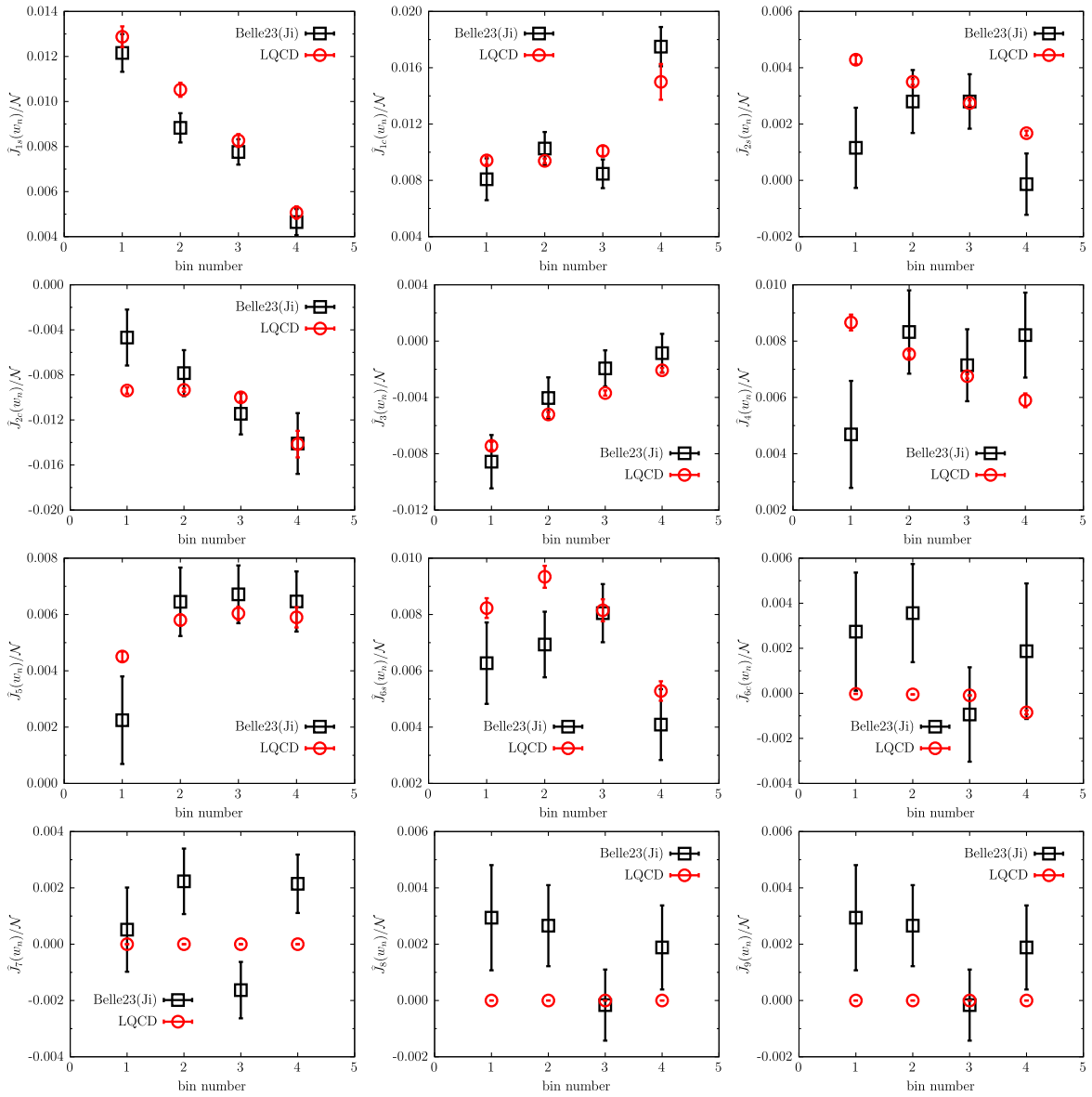

FIG. 3. Normalized angular coefficients $\hat{J}_i(w_n)/\mathcal{N}$, where $\mathcal{N}$ is given in Eq. (15). The red circles represent the SM predictions corresponding to the hadronic FFs of the unitary DM approach of Ref. [21] based on all available LQCD results from Refs. [23–25]. The black squares are the experimental determinations of these quantities as measured by the Belle collaboration in Ref. [17]. The quantities $\hat{J}_7(w_n)$, $\hat{J}_8(w_n)$, and $\hat{J}_9(w_n)$ are exactly zero within the SM.

way the data for the single-differential angular decay rates are evaluated (see the Appendix).

(iii) LQCD: We evaluate the SM predictions for the hadronic parameters (35)–(39) and the helicity amplitudes corresponding to the hadronic FFs obtained by the unitary DM approach in Ref. [21], based on all available LQCD results from Refs. [23–25].[3]

The quality of the fits is acceptable. The values of the reduced χ^2 variable, i.e., $\chi^2/N_{\text{d.o.f.}}$, turn out to be $\simeq 0.3$ (Belle18), $\simeq 1.2$ (Belle23), $\simeq 1.7$ (BelleII23), and $\simeq 1.0$ (Belle18 + Belle23 + BelleII23). The following comments are in order:

(i) The hadronic parameters and the asymmetries extracted from the Belle18 and BelleII23 datasets are consistent within one standard deviation and more precise than those determined from the Belle23 dataset. Differences not exceeding two standard deviations are visible with respect to the Belle23 results.

(ii) The results obtained using simultaneously all three experimental datasets are dominated by the Belle18 and BelleII23 datasets.

[3]Very similar results can be obtained by using the unitary Boyd-Grinstein-Lebed fit, first described in Appendix B of Ref. [28], performed in Ref. [21] on the same LQCD data.

TABLE III. The bin asymmetries $A_{FB}(w_n)$, $F_L(w_n)$, $A_{1c}(w_n)$, and $A_{9c}(w_n)$, evaluated separately in the four w bins of Ref. [17]. Columns 2–5 correspond to the experimental results from Ref. [17], while columns 6–9 refer to the SM predictions corresponding to the hadronic FFs of the unitary DM approach of Ref. [21] based on all available LQCD results from Refs. [23–25]. Within the SM the asymmetry $A_{9c}(w_n)$ is exactly zero.

	Belle23(Ji)				LQCD			
w bin	A_{FB}	F_L	A_{1c}	A_{9c}	A_{FB}	F_L	A_{1c}	A_{9c}
1.00–1.15	0.230 (26)	0.291 (38)	−0.344 (76)	+0.144 (76)	0.230 (63)	0.354 (4)	−0.281 (3)	
1.15–1.25	0.304 (28)	0.449 (35)	−0.188 (68)	+0.041 (68)	0.300 (10)	0.400 (9)	−0.223 (5)	
1.25–1.35	0.292 (29)	0.474 (34)	−0.100 (66)	−0.076 (66)	0.292 (13)	0.475 (16)	−0.174 (8)	
1.35–1.50	0.159 (33)	0.703 (31)	−0.036 (58)	−0.029 (57)	0.180 (15)	0.686 (22)	−0.094 (9)	

(iii) The hadronic parameters and the asymmetries determined using the integrated angular coefficients $\bar{J}_i$ of Ref. [17] turn out to be consistent with those corresponding to the Belle23 dataset within less than one standard deviation. Such small deviations go in the direction of increasing the differences with respect to the results obtained from the Belle18 and BelleII23 datasets.

(iv) The SM predictions based on the hadronic FFs obtained by the unitary DM approach [21] starting from available LQCD results are largely consistent with the results of the Belle23 and Belle23(Ji) datasets (which are not independent), whereas they show some tensions with Belle18 and BelleII23 as well as with the average Belle18 + Belle23 + BelleII23, made over all three experiments, except for the case of the asymmetry A_{1c}.

A visual representation of the above findings, and in particular of the spread between the experimental and theoretical results, is presented in Fig. 2, where the quantities A_{FB}, F_L, and A_{1c} are shown as contour plots that include the correlations among the various quantities.

In Ref. [17] the partially integrated angular coefficients $\hat{J}_i(w_n)$ have been determined in four w bins, namely,

$$\hat{J}_i(w_n) \equiv \int_{w_{n-1}}^{w_n} dw J_i(w), \qquad n = 1, 2, 3, 4, \tag{53}$$

where $\{w_n\} = \{1.0, 1.15, 1.25, 1.35, w_{\rm max}^{\ell}\}$. We may compare the experimental values of $\hat{J}_i(w_n)$ from Ref. [17] with the theoretical predictions obtained from the LQCD FFs from Ref. [21]. The differences between the theory and the experiment, which can be considered only in the case of the Belle23(Ji) data, never exceed a 2σ level. The results are presented in Fig. 3.

After replacing in Eqs. (19)–(23) the quantities $\bar{J}_i$ with the corresponding partially integrated ones $\hat{J}_i(w_n)$, the five hadronic parameters $\{\eta, \eta', \delta, \epsilon, \epsilon'\}(w_n)$ can be determined separately in each of the four w bins of Ref. [17], as well as also the bin quantities $A_{FB}(w_n)$, $F_L(w_n)$, $A_{1c}(w_n)$, and $A_{9c}(w_n)$, corresponding to Eqs. (4)–(7). The results for $A_{FB}(w_n)$, $F_L(w_n)$, $A_{1c}(w_n)$, and $A_{9c}(w_n)$ are collected in Table III and shown in Fig. 4. The experimental results

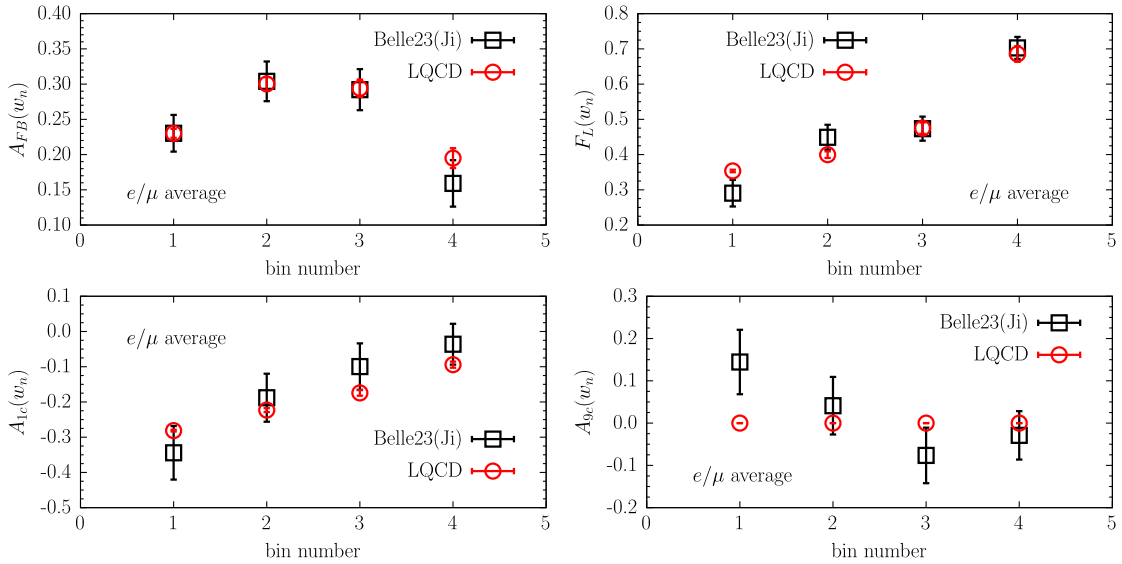

FIG. 4. The bin asymmetries $A_{FB}(w_n)$, $F_L(w_n)$, $A_{1c}(w_n)$, and $A_{9c}(w_n)$, evaluated separately in the four w bins of Ref. [17] (see Table III).

from Ref. [17] turn out to be well consistent with the SM predictions corresponding to the hadronic FFs of the unitary DM approach of Ref. [21], based on all available LQCD results from Refs. [23–25]. The above findings seem to indicate that the w dependence of the experimental angular coefficients $\hat{J}_i(w_n)$ from Ref. [17] is compatible, within $\simeq 2\sigma$, with the slope of the hadronic FFs obtained in Ref. [21] using the available LQCD determinations.

V. CONCLUSIONS

We have presented the results of an analysis of semileptonic $B \to D^* \ell \nu_\ell$ decays based only on the angular distributions of the final leptons. In this way, the problem is reduced to the determination of five basic parameters, which encode in the most general way the contributions to the differential decay rates coming from operators present in the effective Hamiltonian either in the SM or from BSM physics. The analysis is model independent and never requires the knowledge of $|V_{cb}|$.

We have analyzed for the first time the angular distributions of the experimental datasets from Refs. [18,26,27]. This has allowed a direct comparison of the results obtained from different experiments as well as with the theoretical predictions based on the hadronic FFs obtained from LQCD simulations. We have shown that for A_{FB}, F_L, and A_{1c} there are visible differences between different experimental datasets within about two standard deviations (see Fig. 2). Similar differences exist between the SM predictions, based on all the FFs available from LQCD, and some sets of data.

A remarkable good agreement is observed between the experimental data of Ref. [17], given in terms of the angular coefficients $J_i(w)$ [see Eq. (9)], and the SM LQCD predictions, as shown in Figs. 3 and 4. Such a consistency, once confirmed by further experiments, may leave little room to BSM effects in the light lepton sector. In this respect, the forthcoming results from LHCb [29] concerning the coefficients $J_i(w)$ in the case of $B_s^0 \to D_s^* \mu \nu_\mu$ decays will be very valuable.

Finally, we mention that in this work our approach has been applied to the case of the decay data for final light leptons. It can be clearly extended to the case of final τ leptons once experimental data will be available.

ACKNOWLEDGMENTS

The authors warmly thank M. Valli for his valuable help in performing the unfolding of the data of Ref. [18]. S. S. is supported by the Italian Ministry of Research (MIUR) under Grant No. PRIN 2022N4W8WR. The work of L. V. is supported by the French Agence Nationale de la Recherche (ANR) under Contracts No. ANR-19-CE31-0016 ("GammaRare") and No. ANR-23-CE31-0018 ("InvISYble").

DATA AVAILABILITY

No data were created or analyzed in this study.

APPENDIX: THE BELLE23 AND BELLE23(JI) DATASETS

The two datasets Belle23 and Belle23(Ji) share the same raw data for the fourfold differential decay rate, i.e., the lhs of Eq. (9). However, they differ in the way the ratios $(1/\Gamma)d\Gamma/dx$ with $x = \{w, \cos\theta_\ell, \cos\theta_v, \chi\}$ are evaluated.

In the case of Belle23 the ratios have been obtained directly in Ref. [26] by integrating the raw data of the fourfold differential decay rate over three out of the four kinematical variables x.

In the case of Belle23(Ji) two steps are involved. The first one has been performed directly in Ref. [17] and it is the extraction of the angular coefficients J_i obtained by fitting the raw data of the fourfold differential decay rate through Eq. (9) using four w bins. The second step has been performed in this work and it is the evaluation of the ratios (16)–(18) using the integrated angular coefficients $\bar{J}_i$, as described in Sec. IV.

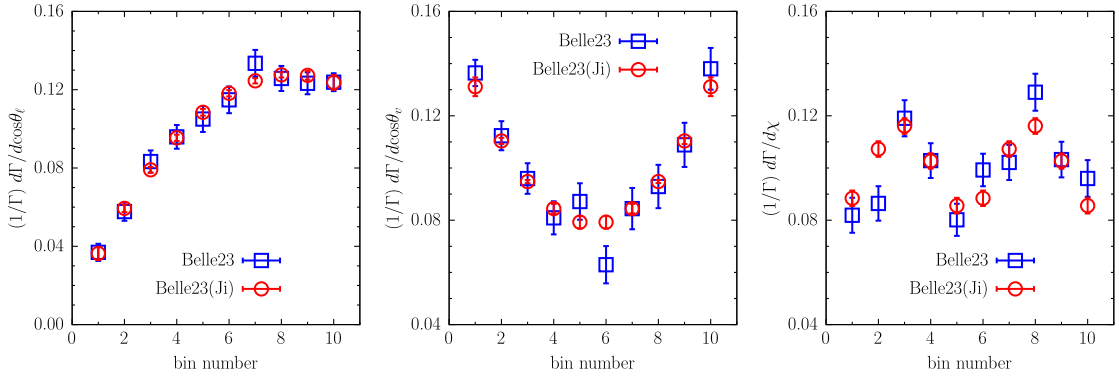

FIG. 5. Ratios $(1/\Gamma)d\Gamma/dx$ for $x = \{\cos\theta_\ell, \cos\theta_v, \chi\}$ corresponding to the two datasets Belle23 and Belle23(Ji). The Belle23 data are directly available from Ref. [26], while the Belle23(Ji) data have been evaluated in this work using in Eqs. (16)–(18) the integrated angular coefficients $\bar{J}_i$, given by Eq. (12), corresponding to the results of Ref. [17].

Note that the uncertainties and correlations of the raw data of the fourfold differential decay rate may have a different impact in the two procedures corresponding to Belle23 and Belle23(Ji). This is confirmed in Fig. 5, where the results for the angular ratios are explicitly shown. The two datasets, Belle23 and Belle23(Ji), are not equivalent for the ratios and, therefore, the values of the extracted hadronic parameters as well as those of A_{FB}, F_L, A_{1c}, and A_{9c} may differ. We stress, however, that, as shown in Fig. 2, the differences in the hadronic parameters corresponding to Belle23 and Belle23(Ji) are well below one standard deviation.

[1] M. Tanaka and R. Watanabe, New physics in the weak interaction of $\bar{B} \to D^{(*)}\tau\bar{\nu}$, Phys. Rev. D **87**, 034028 (2013).

[2] Y. Sakaki, M. Tanaka, A. Tayduganov, and R. Watanabe, Testing leptoquark models in $\bar{B} \to D^{(*)}\tau\bar{\nu}$, Phys. Rev. D **88**, 094012 (2013).

[3] M. Duraisamy and A. Datta, The full $B \to D^*\tau^-\overline{\nu_\tau}$ angular distribution and CP violating triple products, J. High Energy Phys. 09 (2013) 059.

[4] M. A. Ivanov, J. G. Körner, and C.-T. Tran, Analyzing new physics in the decays $\overline{B}^0 \to D^{(*)}\tau^-\bar{\nu}_\tau$ with form factors obtained from the covariant quark model, Phys. Rev. D **94**, 094028 (2016).

[5] P. Colangelo and F. De Fazio, Scrutinizing $\bar{B} \to D^*(D\pi)\ell^-\bar{\nu}_\ell$ and $\bar{B} \to D^*(D\gamma)\ell^-\bar{\nu}_\ell$ in search of new physics footprints, J. High Energy Phys. 06 (2018) 082.

[6] D. Bigi, P. Gambino, and S. Schacht, A fresh look at the determination of $|V_{cb}|$ from $B \to D^*\ell\nu$, Phys. Lett. B **769**, 441 (2017).

[7] M. Jung and D. M. Straub, Constraining new physics in $b \to c\ell\nu$ transitions, J. High Energy Phys. 01 (2019) 009.

[8] S. Jaiswal, S. Nandi, and S. K. Patra, Updates on extraction of $|V_{cb}|$ and SM prediction of R(D*) in $B \to D^*\ell\nu_\ell$ decays, J. High Energy Phys. 06 (2020) 165.

[9] S. Iguro and R. Watanabe, Bayesian fit analysis to full distribution data of $\bar{\mathrm{B}} \to \mathrm{D}^{(*)}\ell\bar{\nu}$: $|\mathrm{V_{cb}}|$ determination and new physics constraints, J. High Energy Phys. 08 (2020) 006.

[10] Z.-R. Huang, E. Kou, C.-D. Lü, and R.-Y. Tang, Un-binned angular analysis of $B \to D^*\ell\nu_\ell$ and the right-handed current, Phys. Rev. D **105**, 013010 (2022).

[11] M. Fedele, M. Blanke, A. Crivellin, S. Iguro, U. Nierste, S. Simula, and L. Vittorio, Discriminating $B \to D*\ell\nu$ form factors via polarization observables and asymmetries, Phys. Rev. D **108**, 055037 (2023).

[12] M. Bordone and A. Juttner, New strategies for probing $B \to D^*\ell\bar{\nu}_\ell$ lattice and experimental data, arXiv:2406.10074.

[13] F. U. Bernlochner, M. Fedele, T. Kretz, U. Nierste, and M. T. Prim, Model independent bounds on heavy sterile neutrinos from the angular distribution of $\mathbf{B} \to \mathbf{D}^*\ell\nu$ decays, arXiv:2410.11945.

[14] C. Bobeth, M. Bordone, N. Gubernari, M. Jung, and D. van Dyk, Lepton-flavour non-universality of $\bar{B} \to D^*\ell\bar{\nu}$ angular distributions in and beyond the Standard Model, Eur. Phys. J. C **81**, 984 (2021).

[15] F. U. Bernlochner, Z. Ligeti, and S. Turczyk, New ways to search for right-handed current in $B \to \rho\ell\bar{\nu}_\ell$ decay, Phys. Rev. D **90**, 094003 (2014).

[16] P. Colangelo, F. De Fazio, F. Loparco, and N. Losacco, New physics couplings from angular coefficient functions of $\bar{B} \to D*(D\pi)\ell\bar{\nu}\ell$, Phys. Rev. D **109**, 075047 (2024).

[17] Belle Collaboration, Measurement of angular coefficients of $\bar{B} \to D*\ell\bar{\nu}\ell$: Implications for $|V_{cb}|$ and tests of lepton flavor universality, Phys. Rev. Lett. **133**, 131801 (2024).

[18] Belle Collaboration, Measurement of the CKM matrix element $|V_{cb}|$ from $B^0 \to D^{*-}\ell^+\nu_\ell$ at Belle, Phys. Rev. D **100**, 052007 (2019); **103**, 079901(E) (2021).

[19] P. Gambino, M. Jung, and S. Schacht, The V_{cb} puzzle: An update, Phys. Lett. B **795**, 386 (2019).

[20] C. G. Boyd, B. Grinstein, and R. F. Lebed, Precision corrections to dispersive bounds on form-factors, Phys. Rev. D **56**, 6895 (1997).

[21] G. Martinelli, S. Simula, and L. Vittorio, Updates on the determination of $|V_{cb}|, R(D^*)$ and $|V_{ub}|/|V_{cb}|$, Eur. Phys. J. C **84**, 400 (2024).

[22] M. Di Carlo, G. Martinelli, M. Naviglio, F. Sanfilippo, S. Simula, and L. Vittorio, Unitarity bounds for semileptonic decays in lattice QCD, Phys. Rev. D **104**, 054502 (2021).

[23] Fermilab Lattice and MILC Collaborations, Semileptonic form factors for $B \to D^*\ell\nu$ at nonzero recoil from $2+1$-flavor lattice QCD, Eur. Phys. J. C **82**, 1141 (2022); **83**, 21 (2023).

[24] HPQCD Collaboration, $B \to D^*$ and $B_s \to D_s^*$ vector, axial-vector and tensor form factors for the full q^2 range from lattice QCD, Phys. Rev. D **109**, 094515 (2024).

[25] JLQCD Collaboration, $B \to D^*\ell\nu_\ell$ semileptonic form factors from lattice QCD with Möbius domain-wall quarks, Phys. Rev. D **109**, 074503 (2024).

[26] Belle Collaboration, Measurement of differential distributions of $B \to D^*\ell\bar{\nu}_\ell$ and implications on $|V_{cb}|$, Phys. Rev. D **108**, 012002 (2023).

[27] Belle-II Collaboration, Determination of $|V_{cb}|$ using $\bar{B}^0 \to D^{*+}\ell\bar{\nu}_\ell$ decays with Belle II, Phys. Rev. D **108**, 092013 (2023).

[28] S. Simula and L. Vittorio, Dispersive analysis of the experimental data on the electromagnetic form factor of charged pions at spacelike momenta, Phys. Rev. D **108**, 094013 (2023).

[29] P. De Simone, F. Manganella, and M. Rotondo, Measurements of the differential distributions of $B_s^0 \to D_s^*\mu\nu_\mu$ decay with the LHCb detector, in *Third Italian Workshop on the Physics at High Intensity (WIFAI 2024)* (Bologna, Italy, 2024), See https://agenda.infn.it/event/41047/contributions/243780/attachments/128157/189756/WIFAI_YSF_Manganella.pdf.